

First plasmas in the TJ-II Flexible Helic

C. Alejaldre, J. Alonso, L. Almoguera, E. Ascasíbar, A. Baciero, R. Balbín, M. Blaumoser, J. Botija, B. Brañas, E. de la Cal, A. Cappa, R. Carrasco, F. Castejón, J. R. Cepero, C. Cremy, J. Doncel, C. Dulya, T. Estrada, A. Fernández, M. Francés, C. Fuentes, A. García, I. García-Cortés, J. Guasp, J. Herranz, C. Hidalgo, J. A. Jiménez, I. Kirpichev, V. Krivenski, I. Labrador, F. Lapayese, K. Likin, M. Liniers, A. López-Fraguas, A. López-Sánchez, E. de la Luna, R. Martín, A. Martínez, L. Martínez-Laso, M. Medrano, P. Méndez, K. McCarthy, F. Medina, B. van Milligen, M. Ochando, L. Pacios, I. Pastor, M.A. Pedrosa, A. de la Peña, A. Portas, J. Qin, L. Rodríguez-Rodrigo, A. Salas, E. Sánchez, J. Sánchez, F. Tabarés, D. Tafalla, V. Tribaldos, J. Vega and B. Zurro.

Asociación Euratom-Ciemat, 28040 Madrid, Spain

D. Akulina, O.I. Fedyanin, S. Grebenschikov, N. Kharchev, A. Meshcheryakov, K.A. Sarksian
General Physics Institute, Moscow, Russia

R. Barth, G. van Dijk, H. van der Meiden
FOM-Instituut voor Plasmafysica 'Rijnhuizen', The Netherlands

S. Petrov
Ioffe Physical Technical Institute, St. Petersburg, Russia

Abstract

First plasmas have been successfully achieved in the TJ-II stellarator using electron cyclotron resonance heating ($f = 53.2$ GHz, $P_{\text{ECRH}} = 250$ kW). Initial experiments have explored the TJ-II flexibility in a wide range of plasma volumes, different rotational transform and magnetic well values. In this paper, the main results of this campaign are presented and, in particular, the influence of plasma wall interaction phenomena on TJ-II operation is discussed briefly.

I. INTRODUCTION

First plasmas have been achieved in the TJ-II stellarator using ECR heating. TJ-II is a low magnetic shear stellarator of the Helic type with an average major radius of 1.5 m and average minor radius of ≤ 0.22 m. The magnetic field ($B_0 \leq 1.2$ T) is generated by a system of poloidal, toroidal and vertical field coils. The central conductors, which provide the flexibility of the TJ-II device, (*i.e.*, its rotational transform and magnetic well depth can be varied over a wide range), consist of a circular coil and two helical coils which are wrapped around the central conductor (Fig. 1). The main characteristics of TJ-II are: a) strong helical variation of its magnetic axis; b) very favourable MHD characteristics with potential for high beta operation; c) operational flexibility and d) bean shaped plasma cross section [1]. The existence of closed and nested magnetic surfaces, in good agreement with the calculated ones, has been demonstrated by magnetic surface measurements made at low magnetic fields [2]. Two gyrotrons (53.2 GHz, up to 700 kW) have been installed for the first stage. The first quasioptical transmission line allows perpendicular power injection while the second one, which is equipped with a movable mirror located inside the vacuum chamber, enables the position of power deposition to be varied while also inducing current by electron cyclotron current drive (ECCD) [3,4]. In a second stage, 2 MW of additional NBI will be available at the beginning of 2000 [5]. Also, a state of the art set of plasma diagnostics, that includes most of the standard systems used in magnetic fusion experiments, is being installed [6]. In addition, a powerful data acquisition system is in operation to handle the large amounts of data (≈ 125 Mbyte/discharge) [7]. The physics programme of the

TJ-II stellarator is focused on transport studies in low collisionality plasmas, operational limits in high beta plasmas, and on studies of transport optimisation and its relationship with the radial electric field.

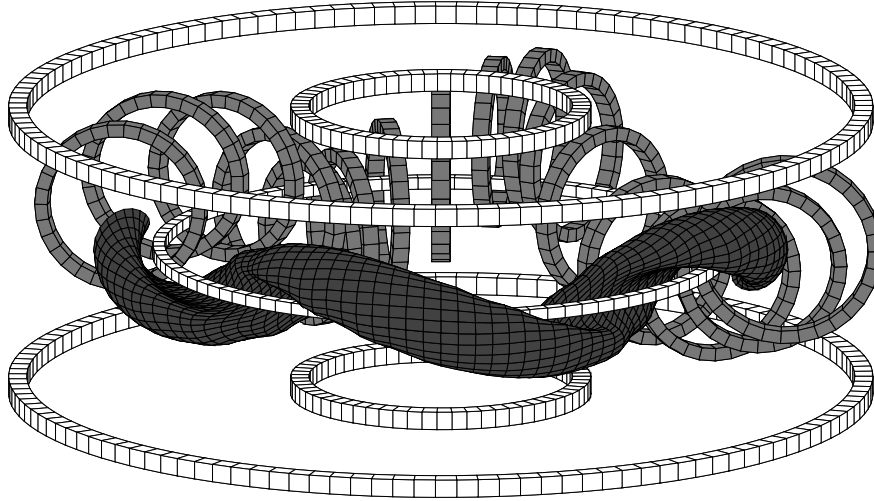


Figure 1: Schematic view of the TJ-II coil system

Characteristics of the ECRH system

The first TJ-II plasmas were obtained using one gyrotron ($f = 53.2$ GHz, $P_{\text{ECRH}} \approx 250$ kW) with a pulse length of $\Delta t \approx (100 - 250)$ ms, and with perpendicular power injection into hydrogen plasmas. The gyrotron is fed by a high voltage power supply that is based on solid state commutative technology. The ECRH output power has a Gaussian-like beam shape. Power is launched into plasmas, through a boron nitride window mounted on the bottom port at the toroidal angle $\phi = 25^\circ$, as an extraordinary wave perpendicular to the magnetic field [8]. The transmission line consists of 8 mirrors of which six are cylindrical mirrors coupled into pairs. The remaining two mirrors are elliptic. A receiving antenna is placed in the transmission line at the edge of the third mirror in order to monitor the microwave power. A power transmission efficiency of 0.9 has been achieved along this mirror line and the wave beam diameter is ~ 10 cm at the plasma border. In addition, a set of receiving antennas has been installed along the TJ-II vessel in order to measure the multi-pass absorption. Measurements show that the residual microwave power that is not absorbed directly by the plasma bulk is absorbed after a few passes through the plasma column. This is in agreement with the extensive linear ray tracing calculations carried out to analyse the performance of the ECRH system in TJ-II [3,4].

Wall conditions

In the experiments reported here, the plasma has been exposed to only metallic (stainless steel) components. According to calculations and to magnetic field mappings (see below), the interaction between the plasma and the vacuum vessel occur mainly in the region surrounding the central coil system, *i.e.*, in the groove. A set of stainless steel plates acts as a thermal shield, thus creating an almost symmetrical helical limiter. Prior to experiments, vacuum levels of $\approx 1 \times 10^{-7}$ mbar are achieved using a set of turbomolecular pumps whose total pumping speed is ≈ 4000 l/s [9]. In the initial phase, room temperature glow discharge cleaning with helium has been used for

wall conditioning. The glow discharge is sustained at a voltage of ≈ 300 V (at $P = 5 \times 10^{-3}$ mbar) between the chamber and two L-shaped anodes. The total discharge current is typically 1 A per anode, equivalent to a current density of $4 \mu\text{Acm}^{-2}$. In future phases, vacuum vessel baking (to 150°) and various coating techniques (such as boronization and lithiation) will be used. Two mobile poloidal limiters have been installed in TJ-II to allow the interaction between the plasma and the vessel to be reduced when required. A set of Langmuir probes and thermoresistances are embedded in the limiters to enable the scrape of layer (SOL) region to be characterised. The influence of poloidal limiters on the SOL thickness and on impurity fueling, as compared with the limiting effect of other parts of the TJ-II vessel (helical limiter), has been studied.

II. CONFIGURATIONAL EFFECTS AND CONFINEMENT STUDIES IN ECRH PLASMAS

Characteristics of the magnetic field and influence of plasma volume on confinement.

The parameters characterising the five configurations considered in this study are shown in Table I. Figure 2 shows the vacuum flux surfaces at the toroidal angle $\phi = 0$ for three configurations. Free boundary equilibria were obtained using a three dimensional equilibrium code (NEMEC).

Name	ι_0	ι_b	Well (%)	Vol(m ³)	R ₀ (%)	R _b (%)
38_38_37	1.50	1.62	2.6	0.337	3.0	18.4
46_46_43	1.60	1.73	4.0	0.560	2.3	24.2
100_32_60	1.42	1.52	2.2	0.934	1.5	32.0
100_40_63	1.51	1.61	2.3	1.065	1.7	35.8
100_50_65	1.61	1.73	2.7	1.260	2.4	40.7

Table I: TJ-II configuration characteristics in the plasma volume scan experiment. R₀ and R_b are the mod(B) ripple at the magnetic axis and at the boundary respectively. The same notation is used for ι .

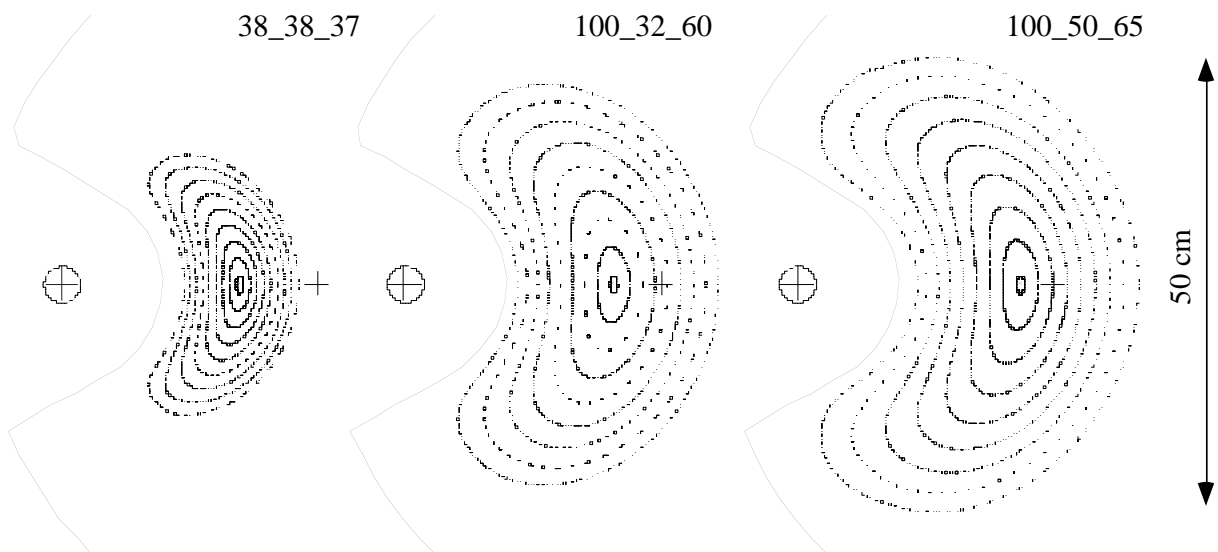


Figure 2: TJ-II vacuum configurations

Plasma configurations with a wide range of plasma volumes, 0.3 - 1.2 m³, and average plasma radius in the range 0.12 - 0.22 m were chosen. The vacuum rotational transform profile is very flat [$\iota(0) - \iota(a) \approx 0.1$] and the magnetic well in the studied configurations is in the range 2 to 4 %. The poloidal location of the plasma-wall interaction in a specific interaction region evolves with the magnetic configurations. Although some degree of toroidal asymmetry is estimated, no hot spots are foreseen in the groove area (helical limiter).

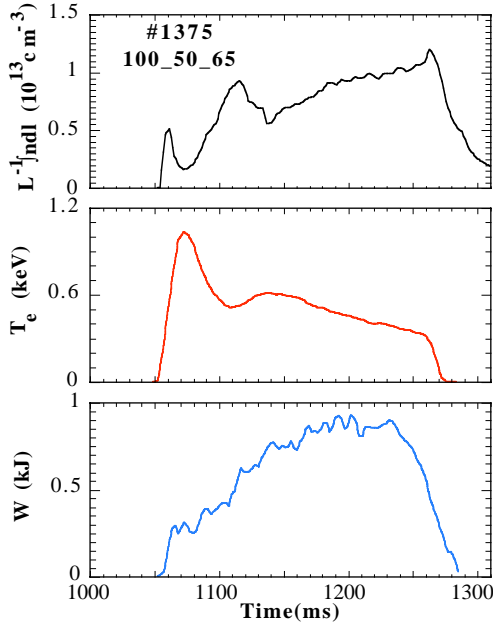


Figure 3: The time evolution of line averaged plasma density, (ECE) central electron temperature and stored energy for a TJ-II magnetic configuration with central $\iota(0) \approx 1.6$ (see table I).

The time evolution of a ECRH discharge is shown in figure 3 for a magnetic configuration with the central $\iota(0) \approx 1.6$. Good conditions for preionization and for plasma start-up by ECRH were achieved by injection of hydrogen at several tens of milliseconds before the gyrotron pulse. Typical pressures were in the 10⁻⁵ mbar range, in agreement with particle balance, and delays between the density built-up and the gyrotron pulse were typically a few milliseconds. Quasi-stationary discharges with the electron cyclotron heating lasting up to 250 ms were obtained. The average electron density achieved was $\langle n_e \rangle \approx 0.5-1.0 \times 10^{19} \text{ m}^{-3}$, the central electron and ion temperatures, T_e and T_i , were ≈ 0.4 to 0.8 keV and $\approx 0.1 \text{ keV}$ respectively, and the stored energy, W , was $\approx 0.8 \text{ kJ}$ (Fig. 3).

Electron temperature profiles obtained from 2nd harmonic ECE and multiposition Thomson scattering system measurements are shown in figure 4 for a series of discharges with $\iota(0) \approx 1.51$. In fact, good agreement is found between the ECE, multiposition Thomson scattering and Si(Li) detector (when available) measurements. The central temperatures are about 600 eV for these discharges. The distortion of the profiles on the low field side of the plasma is interpreted as being caused by a significant population of suprathermal electrons which gives rise to ECE at downshifted frequencies. The edge temperature obtained with edge probes is in the range $T_e(a) \approx 10 - 20 \text{ eV}$. Plasma currents, I , of $\approx 0.5 \text{ kA}$ have been measured, but these appear to be dependent on the location of the plasma resonance (on/off axis heating) which is consistent with ECCD calculations.

Plasma parameter radial profiles have been determined in the plasma boundary region for a range of plasma configurations using fast movable probes and probes installed in movable poloidal limiters. In general, good agreement (within $\pm 0.5 \text{ cm}$) has been obtained between the location of the Last Closed Flux Surface (LCFS) computed from equilibrium codes and the confinement plasma radius taken as the shear layer location, i.e., the point where the electric field changes direction from positive (radially outwards) to negative.

It has been found that global confinement properties are strongly dependent on plasma volume. Figure 5 shows stored plasma energy versus plasma volume. The stored energy increases from 200 J for $V \approx 0.34 \text{ m}^3$ (the smallest plasma configuration), to 1 kJ for $V \approx 1.2 \text{ m}^3$. In the largest plasma configurations, the measured stored plasma energy, W , is $\approx (0.8 - 1) \text{ kJ}$ and the global energy confinement time, $\tau_E^* = W / P_{\text{ECRH}}$, is (3 - 4) ms.

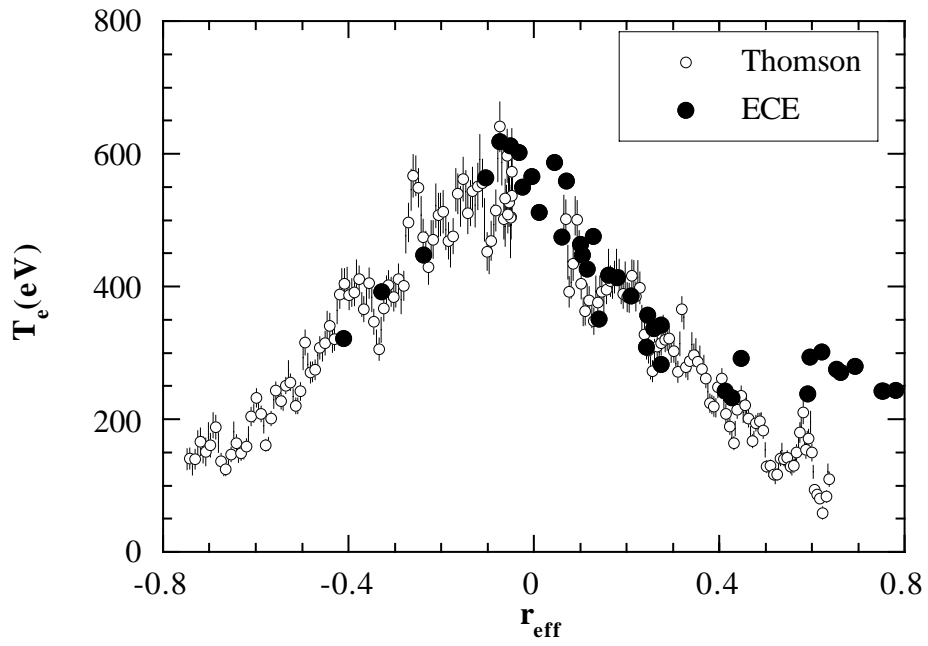


Figure 4: Comparison between electron temperature profiles obtained from 2nd harmonic ECE and Thomson scattering measurements; Thomson data are obtained in a single shot of the discharge series with $iota(0) \approx 1.51$. The maximum that appears on the low field side of the ECE profile is due to the presence of a suprathermal electron population.

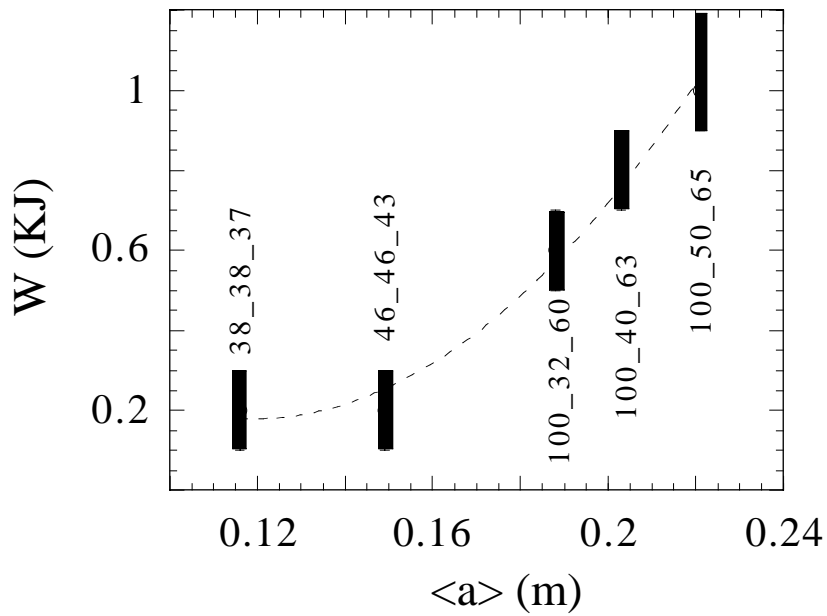


Figure 5: Stored energy versus average plasma radius.

Plasma densities up to the cut-off density ($n_e(0) = 1.75 \times 10^{19} \text{ m}^{-3}$) have been achieved by means of appropriate gas puffing during a plasma discharge. The time decay of the $H\alpha$ signal indicates an effective particle confinement time (τ_p^*) lower than 15 ms for the wall conditions reported here. By considering that all losses are due to the (helical) limiter while assuming that other sources or sinks can be ignored, then the radial flux is given by $\Gamma_{LCFS} \approx 0.5 n(a) c_s \lambda / L_c$, where L_c is the characteristic connection length to the limiter and λ is the e-folding length of particle flux. Field mapping calculations yield $L_c \approx (4 - 5) \text{ m}$ (helical limiter) and probe measurements indicate $\lambda \approx 1.5 - 2 \text{ cm}$ in the upper region of the bean shaped plasma (toroidal angle = 38°). The diffusion coefficient can be described by $D_{SOL} = \Gamma_{LCFS} / \nabla n \approx 1 \text{ m}^2/\text{s}$. This value is close to D_{Bohm} . A density scan has shown that the diffusion coefficient scales roughly with the inverse of edge plasma density. A rough estimation of the global particle confinement time can be obtained from $V n_e / S \Gamma_{LCFS}$, where S is the plasma surface and V the volume. This ratio, which is in the range 5 - 8 ms, is consistent with $H\alpha$ measurements, if allowance for a moderate recycling coefficient is made.

Thomson scattering measurements for different plasma configurations show that the density profile is rather flat whereas the temperature profile is peaked. This result appears to be rather similar to previous studies of plasma profiles in stellarators. The influence of plasma density and collisionality on plasma profiles is currently under investigation.

Rotational transform scan and plasma profiles

An investigation on the influence of natural plasma resonances on plasma profiles and confinement is under way. A magnetic configuration scan has been done to move the 8/5 resonance from the edge to the central region of the plasma. The presence of the natural 8/5 rational surface in the plasma boundary region, as predicted by equilibrium codes for this configuration, has been observed as a flattening in the edge profiles (*i.e.*, ion saturation current and floating potential) (Fig. 6). Interestingly the flattening (with a radial extension of about 1 cm) in density and floating potential profiles is not the same. This is interpreted in terms of the difference in particle and energy transport coefficients in the plasma boundary region. To date, no significant influence of the 8/5 resonance has been observed on global confinement properties. Further experiments are in progress to investigate the influence of major resonances (4/3) on plasma profiles and confinement.

Magnetic well scan and plasma operation

The flexibility of TJ-II allows the magnetic well depth to be modified over at a broad range of values ($\approx 0 - 6 \%$). This high degree of flexibility in the TJ-II device makes it attractive for investigating transport characteristics close to pressure gradient instability thresholds. A preliminary study has been initiated with magnetic configurations having the same rotational transform (iota (0) ≈ 1.8) but with the magnetic well varied from 0.2 to 2%. Figure 7 shows the magnetic well radial profile $[(V'(r) - V'(0))/V'(0)]$ for these configurations. The configuration with the smallest magnetic well (≈ 0.2) has magnetic hill in the outer plasma region ($r/a > 0.7$). Radial electric fields at the plasma boundary region are of the order of 20 V/cm in the plasma configurations with a magnetic well of 6%. In the configuration with the smallest well (≈ 0.2), this becomes $\approx 2 \text{ V/cm}$. Work is underway to study the structure of pressure profiles and fluctuations in configurations with a wide range of magnetic well values.

III. INFLUENCE OF POLOIDAL LIMITER ON PLASMA EDGE STUDIES AND PLASMA OPERATION

The role of the mobile (poloidal) limiters on plasma profiles and their influence on impurity dilution effects has been studied in the plasma configuration with plasma volume of 1.2 m^3 .

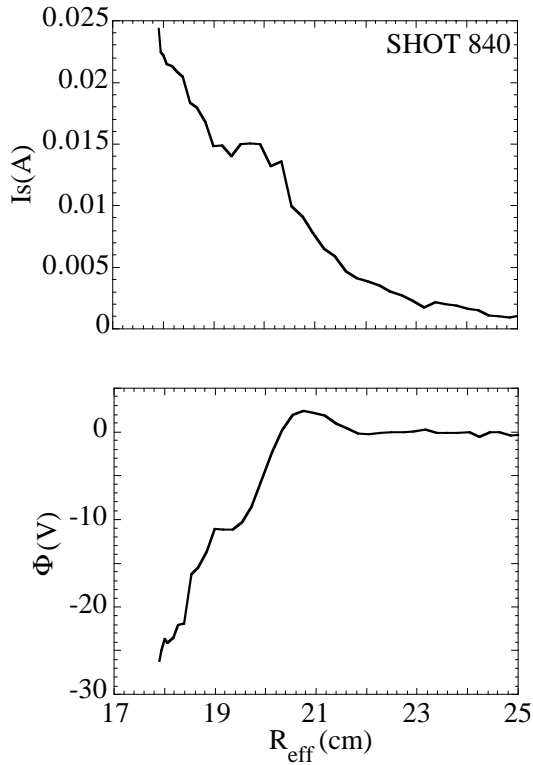


Figure 6: Radial profiles of ion saturation and floating potential in the plasma configuration for $i_0 \approx 1.5$. The flattening of the profile in the plasma boundary region is interpreted in terms of the influence of magnetic islands (8/5) in plasma profiles.

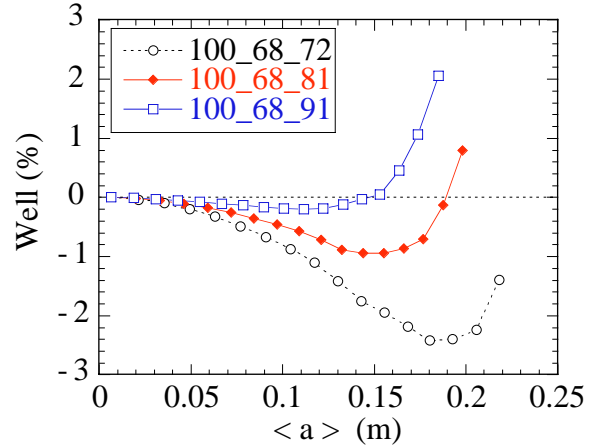


Figure 7: Magnetic well radial profiles for the magnetic configurations investigated in the magnetic well scan experiment.

Field mapping calculations have shown that the characteristic connection length to the poloidal limiter along the flux tube is of 50 m. This value reduces to 3 - 4 m in the case of plasmas with the helical limiter. Radial profiles of ion saturation current and floating potential have been measured for different radial locations of the poloidal limiter. The shear layer location moves inwards as the poloidal limiter is inserted into the plasma edge region and the ion saturation scale length increases. The e-folding length for the ion saturation current increases from 1 cm, when the poloidal limiter is fully removed from the plasma, to 3 cm when the limiting effect of the poloidal limiter is dominant (Fig. 8). This result is in good agreement with field mapping estimates for L_C (*i.e.*, $\lambda \approx L_C^{1/2}$).

A systematic reduction in plasma fuelling by wall impurities is observed as the poloidal limiter is inserted into the plasma, thus permitting a better density control by external gas injection and localised recycling on the mobile limiters.

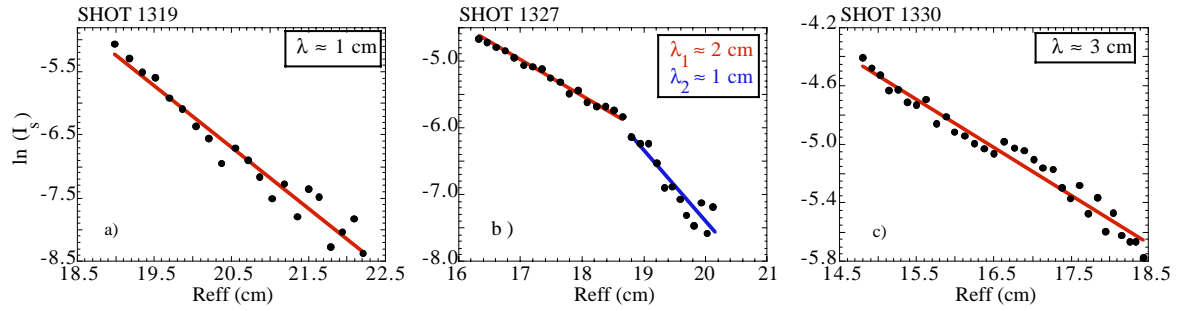


Figure 8: Ion saturation decay lengths for different radial locations of the limiter: (a) the poloidal limiter is located in the proximity of the LCFS computed from equilibrium codes; (b) limiting effect of both poloidal and helical limiters; (c) the limiting effect of the poloidal limiter is dominant.

IV. CONCLUSIONS

The first plasmas of the TJ-II stellarator have been successfully achieved using a 53.2 GHz gyrotron with ECR heating ($P_{\text{ECRH}} \approx 250$ kW). Quasi-stationary discharges lasting up to 200 ms have been obtained with central electron temperatures from 400 to 800 eV, plasma densities $\langle n_e \rangle \approx (0.5 - 1) \times 10^{19} \text{ m}^{-3}$, stored energies in the range 0.2 to 1 kJ and global energy confinement times of up to 4 ms. First experiments have explored the TJ-II flexibility in different plasma volumes and for a wide range of iota and magnetic well values. As expected, in TJ-II, the plasma-wall interaction shows very distinctive features that play an important role in machine operation. An intensive program in first wall conditioning is under development to control the influence of neutrals and radiation on plasma properties.

REFERENCES

- [1] C. Alejaldre et al., *Fusion Technology* 17 (1990) 131.
- [2] E. Ascasibar et al., *J. Plasma Fusion Res. series 1* (1998) 183.
- [3] F. Castejón, C. Alejaldre and J. A. Coarasa, *Phys. Fluids B* 4 (1992) 3689.
- [4] V. Tribaldos, J.A. Jiménez, J. Guasp and B.Ph. van Milligen, *Plasma Phys. Control. Fusion*, (in press) (1998).
- [5] J. Guasp, M. Liniers, C. Fuentes, G. Barrera, *Fusion Technology* (in press) (1999).
- [6] J. Sánchez et al., *Journal of Plasma and Fusion Research series 1* (1998)
- [7] J. Vega, C. Crémy, E. Sánchez, A. Portas, *Fusion Engineering and Design*. (in press) (1998).
- [8] M. Sorolla et al., *Int. Journal Infrared and Millimeter Waves* 18 (1997) 1161.
- [9] F.L. Tabarés et al., *Vacuum* 45 (1994) 1059.